High quality and large-area graphene synthesis with a high growth rate using plasma-enhanced CVD

— Toward a high throughput process —

Masataka HASEGAWA[1,2*], Kazuo TSUGAWA[2], Ryuichi KATO[2], Yoshinori KOGA[2], Masatou ISHIHARA[1,2], Takatoshi YAMADA[1,2] and Yuki OKIGAWA[1,2]

[Translation from *Synthesiology*, Vol.9, No.3, p.124–138 (2016)]

The current trend in graphene synthesis is to use thermal chemical vapor deposition(CVD) at the temperature of 1000 °C or higher. For industrial use of graphene as transparent conductive films, higher throughput of graphene synthesis is necessary. We were among the first to adopt the plasma-enhanced CVD method, and have developed a process of high-speed large-area deposition for transparent conductive film applications. The development and a method to remove impurities from the process are presented in this paper. We report improvement in graphene film quality and other properties by decreasing the nucleus density using plasma-enhanced CVD.

Keywords : Graphene, plasma CVD, large area synthesis, high growth rate, high throughput, transparent electrode

1 Introduction

Graphene[1] is a single atomic sheet in which carbon atoms are arranged in a hexagonal honeycomb lattice. Graphene has a very unique band structure (zero bandgap, linear dispersion), and thereby it shows brilliant electronic and optical characteristics such as extremely high carrier mobility and light absorption which does not depend on wavelength. (2.3 % absorption per layer.) Moreover graphene has the property of flexibility which indium tin oxide (ITO)[2] does not possess, and an attempt has been made to use a few layers of graphene(FLG) as transparent electrodes in such devices as flexible organic light-emitting diode (OLED), solar batteries, and displays.

For transparent electrode application of graphene, it is necessary to establish production technology of high quality and high throughput for large area graphene. Among the various methods of graphene production such as mechanical exfoliation of bulk graphite,[1][3] exfoliation of graphene oxide in liquid phase,[4] thermal decomposition of SiC,[5] etc., chemical vapor deposition (CVD) on catalytic transition metal surfaces, in particular on a copper surface, has great promise as a production method for transparent electrode application. Recently, high conductivity graphene has been synthesized on copper substrates by energetic development of the thermal CVD method.[6][7] On the other hand, since throughput of the thermal CVD method is insufficient, synthesis time needs to be significantly shortened for transparent electrode application. In this paper, we report an attempt to develop high throughput plasma-enhanced CVD for high quality graphene.[8]-[16]

2 Preparation of a substrate for graphene synthesis and suppression of impurity incorporation.

In the case of CVD of graphene using a copper foil substrate, surface cleaning technique of copper foil before CVD is especially important. Also in the case of plasma-assisted CVD (plasma CVD), it is necessary to prevent contamination such as impurities released from the reaction chamber by plasma exposure, particularly silicon, which originate from the quartz of antenna units for exciting plasma.

Commercially available copper foil surfaces are subjected to anticorrosive treatment in order to prevent oxidation. Moreover, even foil with anticorrosive treatment has a surface that is still covered with a thin copper oxide layer. For high-quality graphene synthesis, it is necessary to remove these copper oxide and anticorrosive treatment carefully. In thermal CVD of graphene, electrolytic cleaning and successive high-temperature treatment at about 1000 °C of the copper foil substrate in the reaction chamber are effective for removing copper oxide and the anticorrosive treatment layer. Furthermore, in order to flatten the copper foil surface, chemical polishing (CMP) before electrolytic cleaning and annealing treatment is effective.[17][18] On the other hand, electrolytic cleaning is a wet process and thus there is a possibility of recontamination before CVD. Therefore, cleaning methods consistent with CVD are desirable.

1. Nanomaterials Research Institute, AIST Tsukuba Central 5, 1-1-1 Higashi, Tsukuba 305-8565, Japan ✻E-mail: hasegawa.masataka@aist.go.jp, 2. Technology Research Association for Single Wall Carbon Nanotubes, Graphene Division Tsukuba Central 5, 1-1-1 Higashi, Tsukuba 305-8565, Japan

Original manuscript received March 10, 2016, Revisions received April 27, 2016, Accepted May 26, 2016

In this study, plasma is used, and by establishing plasma cleaning of the surface of the copper substrate, cleaning and synthesis can be carried out continuously in situ. For this reason, it is possible to prevent the recontamination of the substrate.

In many processes using plasma, an inert gas is added to the discharge gas in order to illuminate stably, and argon is commonly used as an inexpensive inert gas. On the other hand, from the point of view of sputtering that causes release of impurities from the reaction chamber, it is desirable to use lighter inert gas.[19]–[21] Thus, we attempted plasma CVD synthesis of graphene using helium, which is expected to be effective for preventing impurity incorporation because of it being the lightest inert gas.

Figure 1 shows a schematic illustration of the surface-wave microwave plasma CVD equipment.[13] The waveguide for microwave propagation is connected to the reaction chamber. The waveguide is equipped with a slot antenna that emits the microwaves into the reaction chamber through a quartz window. In the case of surface-wave microwave plasma, high-density plasma is excited along the surface of the quartz window. High-density plasma which exceeds the cutoff density of 7.4×10^{10} cm^{-3} is excited along the surface of the quartz window by 2.45 GHz microwaves.[22]–[27] Microwaves cannot penetrate through the high density plasma, and the copper foil substrate is not exposed to the microwaves directly. Therefore, temperature control of the substrate is easy over a wide range from low-temperature to high-temperature.[10][11][14]

A tough-pitch copper foil (purity: 99.7 %) with a thickness of 33 μm was used for graphene synthesis. We compared plasma pretreatment of copper foil using two kinds of gas mixtures,

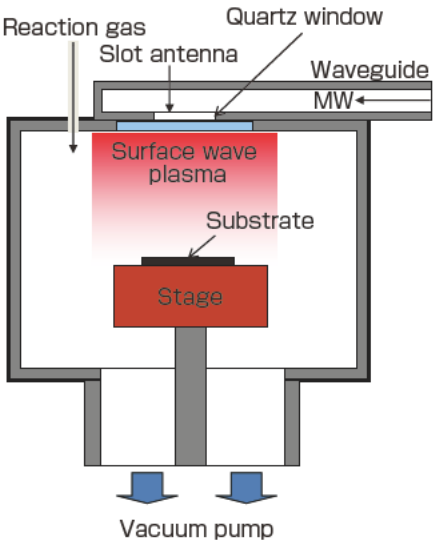

Fig. 1 Schematic illustration of the surface-wave microwave plasma CVD equipment[13]
Copyright (2014) The Japan Society of Applied Physics

Ar/H_2 and He/H_2. The copper foil substrate was placed 50 mm away from the quartz window and the substrate temperature was kept in the range of 350–400 °C. The duration of pretreatment was 1 min. The cleaning effect for the copper foil surface by the plasma pretreatment was confirmed by X-ray photoelectron spectroscopy (XPS) (ULVAC Phi ESCA 5800X, AlKα). XPS measurement was performed ex situ after the cleaning. Quantitative evaluation was considered difficult owing to the oxidation of the copper foil surface by air exposure after cleaning. Therefore, we conducted XPS measurement under the same ex situ condition for all samples and compared the results in terms of the changes in the spectra.

Subsequent to the plasma pretreatment of the copper foil substrate in the reaction chamber, synthesis of graphene by plasma CVD was performed using two kinds of gas mixtures, $He/H_2/CH_4$ and $Ar/H_2/CH_4$. The synthesis time was 20 min. The synthesized graphene films were evaluated by Raman scattering spectroscopy (HORIBA XploRa, spot size 1 μm and wavelength 638 nm), energy-dispersive X-ray spectroscopy (EDS) (JEOL-2100F with EDS detector JED-2300F; acceleration voltage, 200 kV), and XPS. For cross-sectional transmission electron microscope (TEM) observation, an amorphous carbon thin film was deposited on an as-deposited graphene surface in order to make the sample structure robust for gallium focus ion beam etching. TEM observation was performed at an acceleration voltage of 300 keV.

Figure 2 shows the XPS survey spectrum of the as-received tough-pitch copper foil substrate. In this spectrum, the peaks corresponding to Cu 3*d*, 3*p*, 3*s*, 2*p*, and 2*s* and Cu Auger were observed.[28] The peaks of C 1*s* and O 1*s* were also observed together with the low-intensity peaks of Si 2*p* and N 1*s*. It was suggested that these were because organic silicon and hydrocarbon compounds containing nitrogen were coated on the surface of the as-received tough-pitch rolled copper foil. In this study, we examined the removal of these impurities from the copper foil substrate surface by the plasma pretreatment.

In Fig. 3, we compared the XPS high-resolution spectra from the copper foil substrate before and after the plasma pretreatment. First, the removal of copper oxide on the copper foil surface by plasma pretreatment was examined using O 1*s* signals. O 1*s* binding energy spectra are shown in Fig. 3(a). In the case of Ar/H_2 plasma pretreatment, the O 1*s* peak was still observed, which indicates that oxygen was not removed efficiently by this plasma treatment. Moreover, the peaks were separated more clearly, which suggests that a certain amount of oxygen was newly formed during the Ar/H_2 plasma treatment. In contrast, the O 1*s* peak disappeared with the He/H_2 plasma pretreatment, which indicates that the oxygen on the surface was removed efficiently by this plasma

treatment.

Next, we examined the spectrum of Cu 2*p* binding energy shown in Fig. 3(b). For the as-received copper foil substrate, satellite peaks (942.5 eV and 963 eV) attributed to bivalent copper oxides were observed, as well as peaks from Cu 2*p* by orbit-spin coupling and the $2p^{3/2}$ (933 eV) and $2p^{1/2}$ (953 eV) peaks.[29]–[33] The high-energy side of the Cu $2p^{3/2}$ peak of the as-received Cu foil is broad, which is caused by bivalent copper compounds such as $Cu(OH)_2$ and CuO.[29]–[33] In the

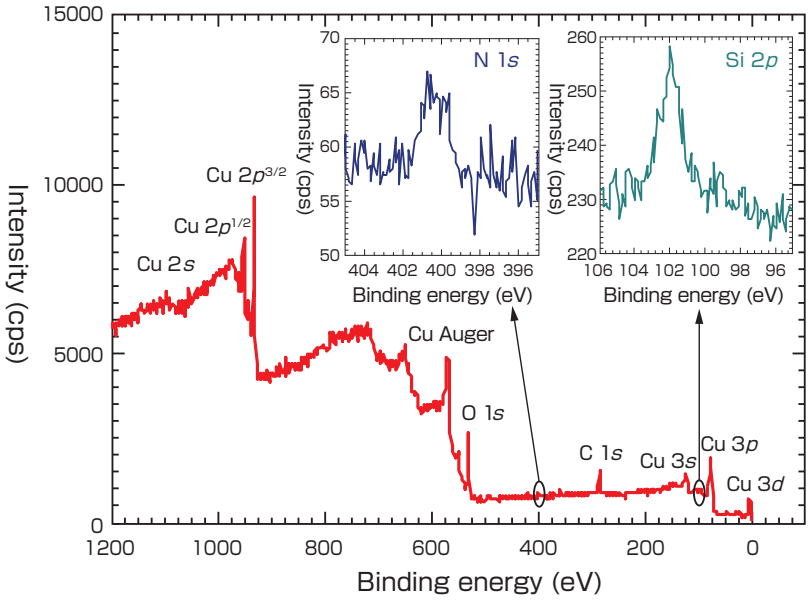

Fig. 2 XPS survey spectrum of the as-received copper foil[13]
Copyright (2014) The Japan Society of Applied Physics

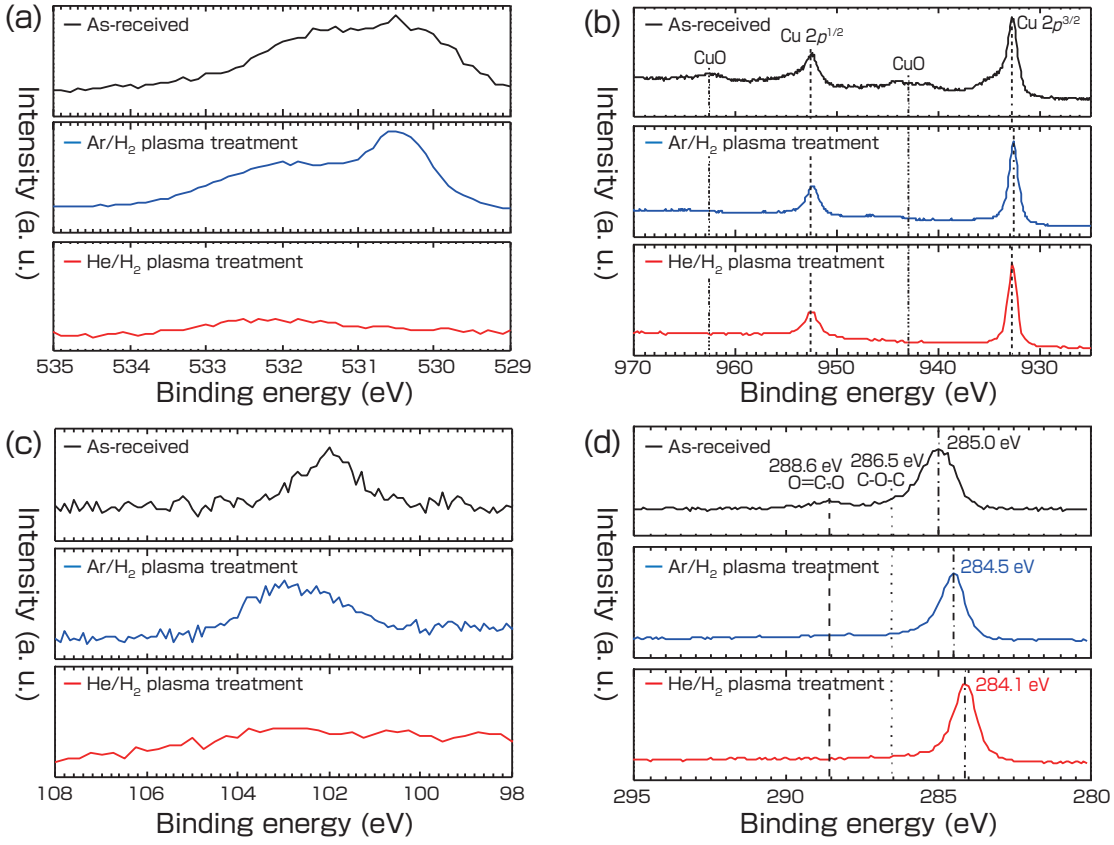

Fig. 3 XPS spectrum of the copper foil with plasma pretreatment and without plasma pretreatment[13]
(a) O 1*s* binding energy, (b) Cu 2*p* binding energy, (c) Si 2*p* binding energy, (d) C 1*s* binding energy
Copyright (2014) The Japan Society of Applied Physics

case of Ar/H_2 plasma pretreatment, the broad peaks (934.5 eV and 942.5 eV) of Cu $2p^{3/2}$ of the bivalent copper oxide compounds disappeared. The peaks due to the monovalent copper oxide Cu_2O still remained in the vicinity of 932.5 eV and 952.5 eV.[29]–[33] From these results, we confirmed that the surface of the as-received copper foil substrate is covered with the bivalent copper oxide on Cu_2O/Cu. The bivalent copper oxide was completely eliminated from the substrate and the monovalent copper oxide was not removed by the Ar/H_2 plasma pretreatment. On the other hand, in the spectrum obtained after the He/H_2 plasma pretreatment, the peaks attributed to monovalent copper oxide, Cu_2O, and the bivalent compounds $Cu(OH)_2$ and CuO were not observed, only the peaks attributed to Cu $2p^{1/2}$ and Cu $2p^{3/2}$ of pure copper were observed. This is consistent with there being no O 1*s* signals related to any oxides on the copper foil substrate after the He/H_2 plasma pretreatment, as shown in Fig. 3(a). This indicates that the He/H_2 plasma pretreatment is very effective for removing copper oxide on the surface of copper foil substrates.

Then, we examined the removal of silicon impurities on the copper foil substrate from the XPS spectrum of the Si 2*p* binding energy shown in Fig 3(c). A peak with Si 2*p* binding energy of 102 eV was observed on the surface of the as-received copper foil substrate. We surmise that siloxane compounds containing Si, such as silicone were applied as protective coating for copper foil surfaces before shipment from the factory. The Si 2*p* binding energy of Si compounds depends on the oxidization state of siloxy units[34][35] and silicon oxides.[36] If the number of oxygen atoms binding to Si atoms increases, the Si 2*p* binding energy will shift from 101 eV to 103 eV. The observed binding energy of 102 eV of Si 2*p* corresponds to that of poly(dimethylsiloxane) (PDMS),[34][35] as shown in Fig. 3(c). In the case of Ar/H_2 pretreatment, a new peak at 103.0 eV due to Si 2*p* appeared, although the peak intensity of Si 2*p* at 102.0 eV of the as-received copper foil substrate decreased slightly. The appearance of the peak of Si 2*p* at 103.0 eV following the Ar/H_2 plasma pretreatment occurs for two reasons. First is the oxidation of PDMS, indicating the formation of a CH_3SiO_3 siloxy unit by the oxidization of the CH_3SiO_2 (PDMS), as shown in Fig. 3(c). Second is the formation of SiO_2 from etching of the quartz window by the Ar/H_2 plasma. In contrast, the peak due to Si 2*p* disappeared completely after the He/H_2 plasma pretreatment. Hence, it is found that the He/H_2 plasma pretreatment effectively eliminates silicon impurities including silicon oxides on the copper foil surface and suppresses the extreme over-plasma etching of the quartz window.

Furthermore, we investigated the XPS spectrum of the C 1*s* region in order to clarify the protective coating material on the as-received copper foil substrate, as shown in Fig. 3(d). There are three peaks at 285.0 eV, 286.5 eV, and 288.6 eV observed for the as-received copper foil. The strongest peak observed at 285.0 eV is mainly due to the C-C and C-H bonded groups in a sp^3-hybridized state.[37] The shoulder peak observed at 286.5 eV is due to C-O-C bonding of the ether/phenolic components, and the highest binding energy observed at 288.5 eV is due to O=C-O bonding of the ester/carboxylic components.[37] Furthermore, we observed nitrogen atoms at 400.2 eV in the inset of the survey spectrum in Fig. 2. Again, we surmise that this is due to a corrosion inhibitor for copper foil that contains O=C-O, C-O-C, C-C, and C-H groups and N. It is well known that benzotriazole (BTAH) is used as an effective corrosion inhibitor for copper.[38][39] Although, BTAH ($C_6H_5N_3$) has none of the functional groups of O=C-O and C-O-C, Finšgar *et al.* have observed the XPS C 1*s* spectrum with these groups on the surface of copper after of 1 h treatment with 3 % NaCl solution containing 10 mM BTAH.[38] They suggested that either the oxidation of carbonaceous species occurred or oxidized carbon compounds were adsorbed on the topmost surface of copper. Their spectrum closely resembles that of the as-received copper foil in Fig. 3(d). They have also observed signals of the Cu Auger $L_3M_{4,5}M_{4,5}$ region of the Cu-BTAH complex at 572.6 eV at uppermost part of the copper substrate using angle resolved XPS measurement. The signal of the Cu-BTAH complex in the region of Cu Auger was not detected in our experiment, because it was not an angle-resolved measurement.

After the Ar/H_2 plasma pretreatment, the peak of C 1*s* at 285 eV observed for the non-plasma-treated substrate became sharper and the peaks at 288.6 eV and 286.5 eV disappeared. This means that BTAH is easily decomposed by the Ar/H_2 plasma pretreatment. The peak of C 1*s* at 285.0 eV shifted to 284.5 eV after the Ar/H_2 plasma pretreatment. The binding energy of 284.5 eV corresponds exactly to that of PDMS.[35] Hence, PDMS was mostly left on the copper foil substrate after the Ar/H_2 plasma pretreatment. This is consistent with the existence of PDMS of O 1*s* (532.0 eV) in Fig. 3(a) and Si 2*p* (102.0 eV) in Fig. 3(c) after the Ar/H_2 plasma pretreatment. After the He/H_2 plasma pretreatment, the binding energy observed at 284.1 eV corresponds to that of HOPG which is composed of sp^2 bonding.[40][41] These were confirmed as amorphous sp^2 carbon films from the Raman spectrum.

The difference between the effect of He/H_2 and Ar/H_2 plasma pretreatment methods can be attributed to the difference between the sputtering yields of SiO_2 for helium and argon. In the case of surface-wave plasma CVD, high-density plasma is excited in the vicinity of the quartz window, and the mixing of silicon and oxygen with the plasma by the sputtering of the quartz window is a major issue. That is, it is necessary to suppress the deposition of such impurities onto the substrate. According to the basic theory of sputtering by Sigmund, sputtering yield depends on the atomic weight and atomic number of the target and ions.[20] When the ion energy is 100–600 eV, the yield of quartz (SiO_2) sputtering with argon ions is 2.5–3.8 times greater than that of helium ions.

Furthermore, the molecular dynamics simulation of energetic ion bombardment of He^+, Ne^+, Ar^+, Kr^+ and Xe^+ for SiO_2 have also been reported.[21] The sputtering yield for SiO_2 substrates increased along with the atomic number of impact ions. The lightest He^+ among these ions could not efficiently transfer its energy to surface atoms on the SiO_2 substrate even at ion energy of 100 eV, and the sputtering yield by He^+ was almost zero. On the other hand, Ar^+ effectively showed sputtering of SiO_2.[21] Therefore, it was shown that it was possible to suppress the deposition of silicon and oxygen from the quartz window onto the copper foil substrate by the He/H_2 plasma pretreatment, and the cleaning of the copper foil surface could be performed effectively.

The syntheses of graphene by $Ar/H_2/CH_4$ and $He/H_2/CH_4$ plasma CVD on a copper foil substrate pretreated with Ar/H_2 and He/H_2 plasma was examined and compared with that without such pretreatment. The Raman spectra of the synthesized graphene by plasma CVD are shown in Fig. 4. The G-band (1520 cm^{-1}) overlapping with the D'-band and the D-band (1320 cm^{-1}) were observed for the as-received copper foil substrate prepared by $He/H_2/CH_4$ plasma CVD. However, the 2D-band was not observed on the as-received substrate prepared without plasma pretreatment. In the case of $Ar/H_2/CH_4$ plasma CVD subsequent to the Ar/H_2 plasma pretreatment, the 2D-band (2650 cm^{-1}) was observed with half the intensity of the G-band. In the case of $He/H_2/CH_4$ plasma CVD subsequent to the He/H_2 plasma pretreatment, the 2D-band (2650 cm^{-1}) was observed with the same intensity as the G-band. This result, combined with the result of the cross-sectional TEM image, indicates that the crystalline of graphene synthesized using $He/H_2/CH_4$ plasma CVD at low-temperature (350–400 °C) on a He/H_2 plasma pretreated copper foil substrate is better than that synthesized on an Ar/H_2 plasma pretreated substrate, as will be described later. That is, it suggests that the He/H_2 plasma pretreatment successfully removes copper oxide and impurities on the substrate surface and recovers the catalytic effect of the copper surface for graphene synthesis. In plasma CVD of graphene, the synthesis is completed within several tens of seconds, and has the potential to synthesize graphene in a short time. In order to realize the continuous synthesis of high-quality graphene of high-throughput, it is necessary to sufficiently remove the oxide and contaminations prior to the synthesis.

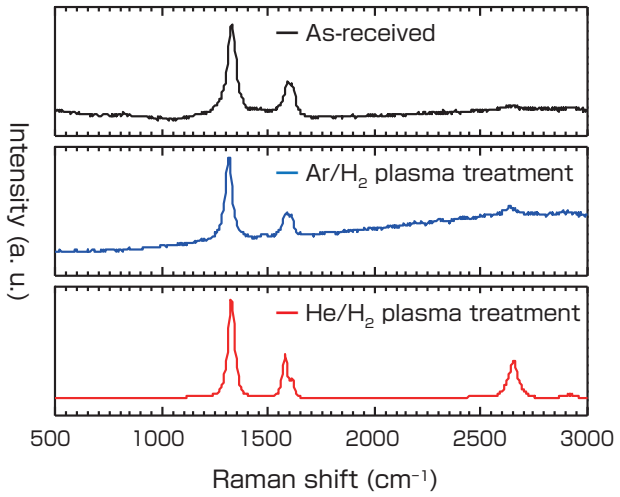

Fig. 4 Raman spectrum of graphene synthesized on the copper foil substrate[13]

Figure 5 shows a comparison of the details of the spectra at around Si 2*p* binding energy for graphene films synthesized using $He/H_2/CH_4$ and $Ar/H_2/CH_4$ plasma CVD. The Si 2*p* (103.0 eV) was observed clearly in the spectrum of the graphene film synthesized by $Ar/H_2/CH_4$ plasma CVD, but not in the spectrum of that synthesized by $He/H_2/CH_4$ plasma CVD. In order to obtain more detailed information with respect to the impurities contained in the graphene film, an elemental analysis of very thin (one or two layers) films was conducted by EDS (Fig. 6). In the case of the synthesized graphene film using $Ar/H_2/CH_4$ plasma CVD, about 2 % silicon was detected, whereas less than 0.8 % silicon including the background signals was detected in the graphene film synthesized using $He/H_2/CH_4$ plasma CVD. Therefore, from the results of impurity analysis of XPS and EDS, it is concluded that the incorporation of silicon from

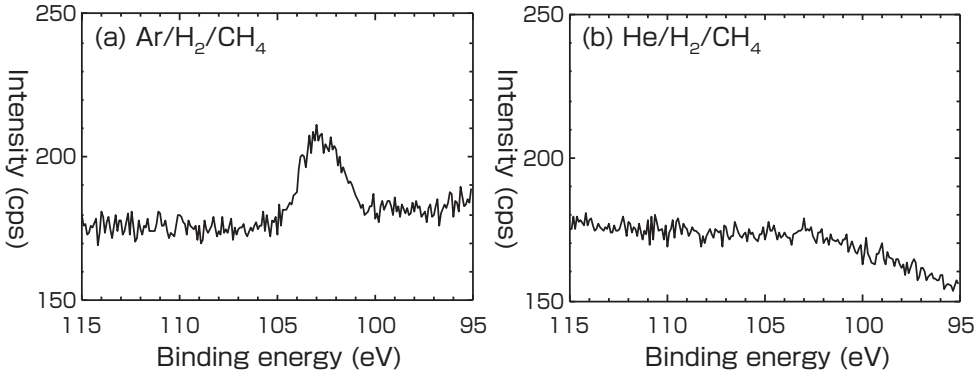

Fig. 5 XPS spectrum of Si 2*p* binding energy for synthesized graphene using (a) the $Ar/H_2/CH_4$ gas mixture and (b) the $He/H_2/CH_4$ gas mixture[13]

the quartz window onto the synthesized graphene film is suppressed more effectively by $He/H_2/CH_4$ than $Ar/H_2/CH_4$.

As in the pretreatment of the substrate, mixed gas using helium or argon for plasma CVD results in a significant difference between the synthesized graphene films. Figure 7 shows the comparison between the cross-sectional TEM images of graphene films synthesized using (a) $He/H_2/CH_4$ and (b) $Ar/H_2/CH_4$ mixed gases. In the case of mixed gas of helium, a multilayer graphene film consisting of 20 layers was synthesized directly on the copper foil substrate by CVD for 20 min. The layer spacing was 0.34 nm, which is slightly larger than 0.335 nm of graphite. In the thermal CVD on the copper foil substrate, the growth of graphene is limited to two or three layers.[6] In contrast, in the case of plasma CVD of graphene, a much thicker film is grown on the copper foil substrate as shown in this example. This is one of the remarkable features of this method. In the case of mixed gas of argon, on the other hand, the diagonal layered structure in the cross-sectional TEM image was confirmed on the copper foil substrate. A layer spacing of 0.27–0.28 nm, which corresponds to that of CuO(110), indicates the formation of the copper oxide layer during $Ar/H_2/CH_4$ plasma CVD. Along the surface of the copper oxide layer, a weak contrast of the layered structure was also confirmed. The layer spacing of 0.34–0.37 nm, however, is much larger than that of graphite, which suggests that the synthesized graphene layer was partly oxidized like the copper foil substrate.

In this research we developed a plasma pretreatment method for copper foil substrates, and a plasma CVD method for high-quality graphene by suppressing the impurity incorporation onto the graphene surface. It is found that the plasma pretreatment using He/H_2 removes copper oxide on the surface more effectively than using Ar/H_2, and is also effective for preventing the substrate from being contaminated by silicon impurities attributed to the sputtering of the quartz window. The plasma pretreatment of the copper foil substrate using He/H_2 is found to improve the crystalline of synthesized graphene. The incorporation of silicon impurities from the quartz window onto synthesized graphene films is suppressed using $He/H_2/CH_4$ more effectively than using $Ar/H_2/CH_4$.

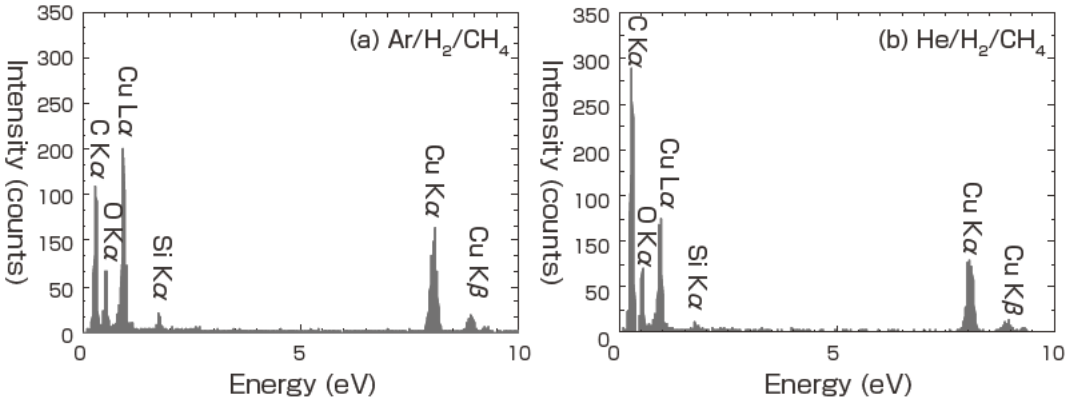

Fig. 6 EDX spectrum of Monolayer and/or bilayer graphene synthesized using (a) the $Ar/H_2/CH_4$ gas mixture and (b) the $He/H_2/CH_4$ gas mixture[13]

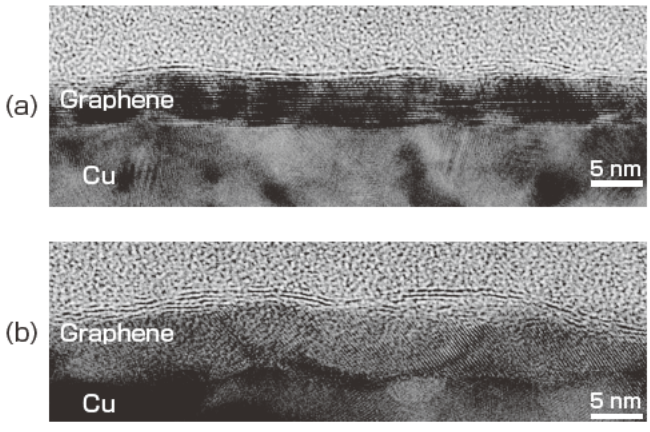

Fig. 7 Cross-sectional TEM images of synthesized graphene by surface-wave plasma using (a) the $He/H_2/CH_4$ gas mixture and (b) the $Ar/H_2/CH_4$ gas mixture[13]

3 A development of plasma CVD using ultralow carbon source

For the industrial application of graphene transparent conductive films, establishment of a synthesis method of high-quality and high-throughput is required. As described previously, the synthesis of graphene by CVD on transitional metal substrates (in particular on copper) is the most promising at the moment.[6] Currently, transmittance of 90 % (four-layers stacking) in the region of visible wavelength and sheet resistance of 30 Ω are indicators of high-performance graphene synthesized by thermal CVD.[7] A demonstration of an organic light-emitting diode (OLED) with graphene anodes which has higher luminous efficiency than by using ITO has been reported.[42] Since visible light transmittance of 90–93 % is required for the transparent electrode application of graphene, three or four layers of graphene are necessary. Hence, it is important to improve the controllability of the graphene synthesis for multilayers as well as a single layer.

For the realization of the mass production of graphene by a roll-to-roll method, it is required to reduce the thermal load on the apparatus and to attain a significant reduction of synthesis time. An attempt was made to reduce the thermal load on the apparatus by direct joule heating of the copper foil substrate and to demonstrate roll-to-roll thermal CVD synthesis of graphene at 950 °C by the Sony group.[43] In this example, winding speed of the copper foil substrate was 1.5 mm/sec, and further increase of speed is desired for high-throughput production. Also in order to suppress the microcracks due to thermal expansion and thermal contraction of the copper foil to improve the quality of the graphene, further reduction of the temperature is required.

We have developed plasma CVD of graphene to reduce the process temperature and the process time at the same time. By combining low temperature surface-wave plasma CVD with roll-to-roll transfer of copper foil substrate, high-throughput synthesis of graphene with winding speed of 5–10 mm/s was demonstrated by the AIST group.[9][10] The problem of plasma CVD of graphene is the crystal size (domain size) of 10 nm or smaller, which inhibits electrical conductivity. By the large growth rate and high nucleation density of plasma CVD, graphene growth in the two-dimensional direction is prevented, which causes stacking of small flakes in multiple layers and deterioration of the controllability of the number of layers.

In this study, we attempted to expand the size of graphene crystals and to improve the controllability of the number of layers by reducing the concentration of the carbon source used for graphene synthesis which is expected to suppress the nucleation density. Without supplying carbon-containing gas such as methane, as an ultralow concentration of carbon source, we utilized trace amount of carbon contained in the copper foil and/or supplied from the environment in the reaction chamber. We attempted to expand the crystal size of graphene and improve the electrical conductivity by developing this method. Moreover, we attempted to synthesize AB-stacked bilayer graphene with good controllability in a high yield. This method combines joule heating and hydrogen plasma treatment for the copper foil substrate and it is aimed at the establishment of an industrially advantageous method at lower temperature and requiring shorter time as compared to the conventional thermal CVD method.

First of all, we performed only heat treatment at each temperature of 300, 400, 600, 800, and 1000 °C of the copper foil by using direct joule heating in 20 Pa hydrogen for 15 min in the reaction chamber and the foil was cooled down to room temperature. The size of the heat treated sample was 6 × 6 mm^2. A copper foil heated at each temperature was examined by Raman spectroscopy (Model: HORIBA XploRa, beam spot of 1 μm in diameter, excitation laser of 632 nm wavelength). It was tested whether graphene was synthesized by only the joule heat treatment in a hydrogen atmosphere as shown in Fig.8.

Hydrogen plasma treatment was performed in 30 sccm flow and 5 Pa for 30 s. The surface-wave microwave plasma with low electron temperature which was expected to reduce the ion bombardment was utilized for plasma treatment.

The synthesized graphene was transferred to a transparent polymer substrate to measure the electrical conductivity and the optical transmittance. The slightly-adhesive resin film was used as the transparent polymer substrate. The thickness of the resin film was 41–42 μm. After bonding the resin film and copper foil with graphene onto the surface of the copper foil substrate, the copper foil was removed by etching using an aqueous solution of ammonium persulfate (0.50 mol/ℓ).

The electrical characteristic of the synthesized graphene

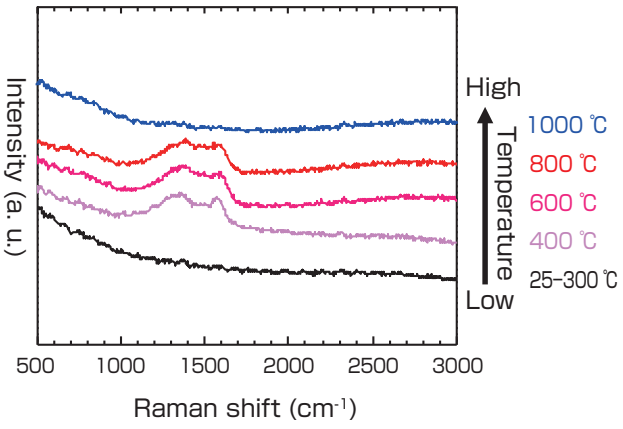

Fig. 8 Raman spectrum of the copper foil heated from room temperature up to 1000 °C at hydrogen atmosphere[14]
Copyright (2014), with permission from Elsevier

was measured at 36 points by a four probe method for sheet resistance using gold alloy probes at 1 mm mesh over the sample area of 6 × 6 mm^2. The carrier mobility was estimated by Hall effect measurement in Van der Pauw geometry.[44]

Next, the transferred graphene on the polymer substrate was immersed in an isopropyl alcohol solution of gold chloride (20 mol/ℓ), and dried.

Figure 8 shows the Raman spectra of copper foil observed at room temperature after only the joule heating treatment in a hydrogen atmosphere. Although carbon-related signals in the Raman spectrum were not observed within the detection limit for the heat treatments lower than 300 °C, the spectra of copper foil subjected to the heat treatment at 400, 600, and 800 °C indicated the formation of amorphous carbon films[45] on the surface. Since carbon-containing gas such as methane was not introduced, there should be alternative carbon sources such as one dissolved in the copper foil and/or one supplied from the environment inside the reaction chamber.

The concentration of impurity carbon in the copper foil was examined by a combustion method, which has been estimated to be 5–31 ppm. The areal density of carbon atoms in graphene is $3.8\times10^{15}/cm^2$. If a graphene sheet with the highest impurity carbon concentration of 31 ppm is used, copper foil of 15 μm thickness is at least necessary to supply the carbon atoms to synthesize single layer graphene. Because the thickness of the copper foil in the present study was 6.3 μm, carbon atoms supplied from the environment in the reaction chamber must have been from an additional or main source of carbon atoms. The base pressure of the reaction chamber, which was evacuated by using oil-free turbo molecular pump system, was lower than 1.0×10^{-4} Pa. It was not clarified which was the main supplier of carbon, the copper foil or the environment in the reaction camber. In this paper, the discussion is based on both having the possibility.

The copper foil substrate was treated by the joule heating treatment of temperatures up to 1000 °C in hydrogen atmosphere without supplying any carbon gas sources. Raman spectra were measured at room temperature after the cooling of the copper foil substrate in a hydrogen atmosphere. As shown in Fig. 8, however, we could not observe the Raman peaks which indicate the graphene formation on the copper surface. The peaks from amorphous carbon at 1350 cm^{-1} and 1580 cm^{-1} were lost by the heating at 1000 °C. It was considered that it was because heat treatment was conducted at temperature close to the melting point of copper (1085 °C) under low pressure, and the precipitated carbon atoms decomposed or were lost with the evaporation of the copper foil surface.

Therefore, although amorphous carbon precipitation was observed at 400, 600, and 800 °C, there were no Raman signals on the copper substrate pretreated at the temperature between 25 °C and 300 °C, and 1000 °C.

A Raman spectrum for only hydrogen plasma treatment for 30 s without heat treatment of copper foil is shown in Fig. 9(a). In this case, no peaks attributed to carbon related materials such as graphene and amorphous carbon were observed. Figure 9(c) shows a Raman spectrum from copper foil subjected to hydrogen plasma treatment for 30 s subsequent to the treatment by joule heating at 1000 °C. Although, the very weak G-band ($1580cm^{-1}$) and the D-band ($1350\ cm^{-1}$) were observed, the 2D-band in the range of 2641–$2681\ cm^{-1}$ was not observed. This indicated that graphene was not formed at this temperature because an extremely small amount of carbon supply disappeared along with the evaporation of the copper foil substrate. Figure 9(b) shows Raman spectra from the copper foil substrate subjected to hydrogen plasma treatment for 30 s at 850 °C subsequent to the treatment by joule heating at 850 °C. Distinct G-band and 2D-band were observed with very low intensity of the D-band which indicated low defect.

Then, since in Fig. 9(b) it was shown that the 2D-band has different line width and intensity distribution, we analyzed it in more detail. As shown in Fig. 10, two kinds of graphene which have different full width at half maximum (FWHM) of the 2D-band were observed. We analyzed the 2D-band at 46 points in 12 samples which were synthesized under the same conditions using the curve fitting by a single Lorentzian peak and the sum of four single Lorentzian peaks as shown in Fig. 10(a) and (b), respectively, according to the fitting

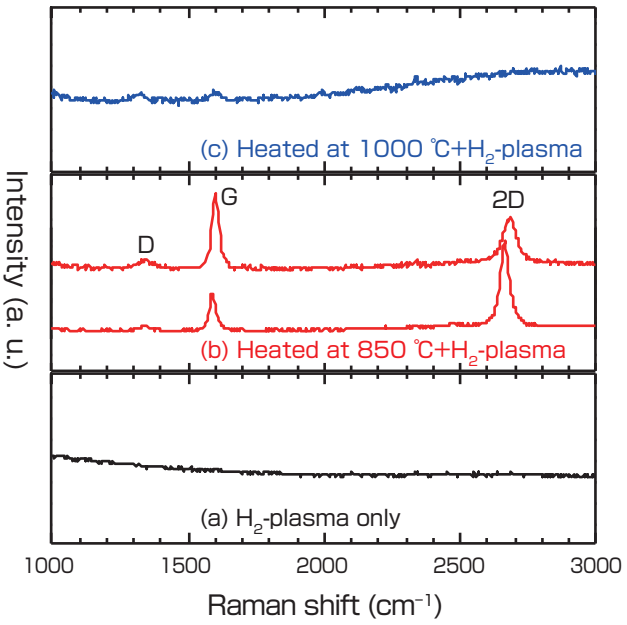

Fig. 9 Raman spectrum of the copper foil after hydrogen plasma treatment[14]
(a) only hydrogen plasma, (b) hydrogen plasma while heating at 850 C, and (c) hydrogen plasma while heating at 1000 C

method cited in References [46] and [47]. AB-stacked bilayer graphene is fitted by the sum of four Lorentzian peaks of the 2D-band with FWHM from 41.0–59.5 cm^{-1} (Fig. 10(a)). On the other hand, a disoriented stacked bilayer graphene is fitted by a symmetric single Lorentzian peak with FWHM of 36.0–40.5 cm^{-1} (Fig. 10(b)).

To examine the yield of AB-stacked bilayer and disoriented bilayer graphene, histograms of FWHM values of the 2D-band and Raman intensity of the 2D-band/G-band ratio are shown in Fig. 11. In the case of Raman intensity ratio (2D-band/G-band), the range of 0.7–2.7 is for AB-stacked bilayer graphene and 2.8–5.1 is for disoriented bilayer graphene. These results indicate a graphene yield of 60 % of AB-stacked bilayer graphene and 40 % of disoriented bilayer graphene on the copper foil substrate synthesized by hydrogen plasma treatment during heat treatment by joule heating. The D-band (1338cm^{-1}) due to the defects in graphene crystal was observed with very weak intensity. With the identification of the number of layers and the stacked structure by Raman spectroscopy, single layer graphene and trilayer graphene were not observed in all samples synthesized by this plasma treatment condition. The crystal size of graphene was about 100 nm by estimated Raman intensity D-band/G-band ratio. (Described later) While the crystal size of synthesized graphene by using carbon source gas of the previous method was less than 10 nm, it is possible to definitely improve the crystal size by plasma CVD using a carbon source of ultralow concentration of the present method. In addition, it is suggested that this method is quite suitable for industrial continuous production such as the high-throughput roll-to-roll method from the point of view of very short process time and high growth rate.

Then, the synthesized graphene in this study was transferred to a slightly-adhesive resin film in order to measure the optical transmittance. Fig. 12 shows the optical transmittance

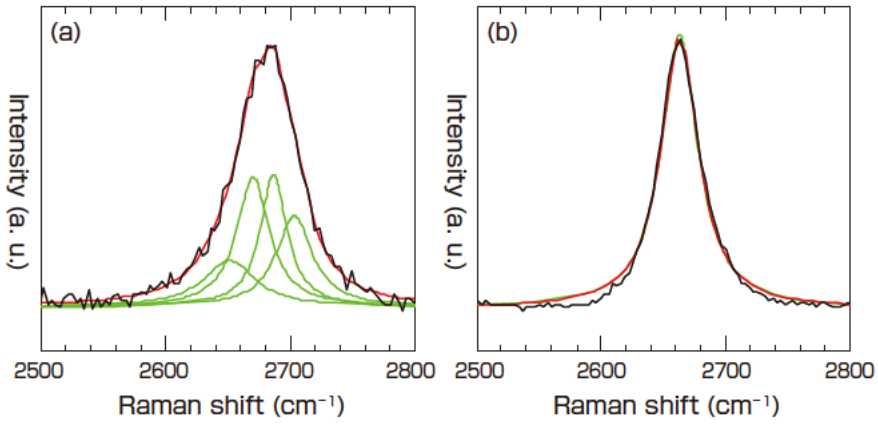

Fig. 10 Raman spectrum fitting analysis of 2D-band[14]
(a) AB-stacked bilayer graphene which fits sum of four Lorentzian peaks, and (b) disorder-stacked bilayer graphene which fits the symmetric peak
Copyright (2014), with permission from Elsevier

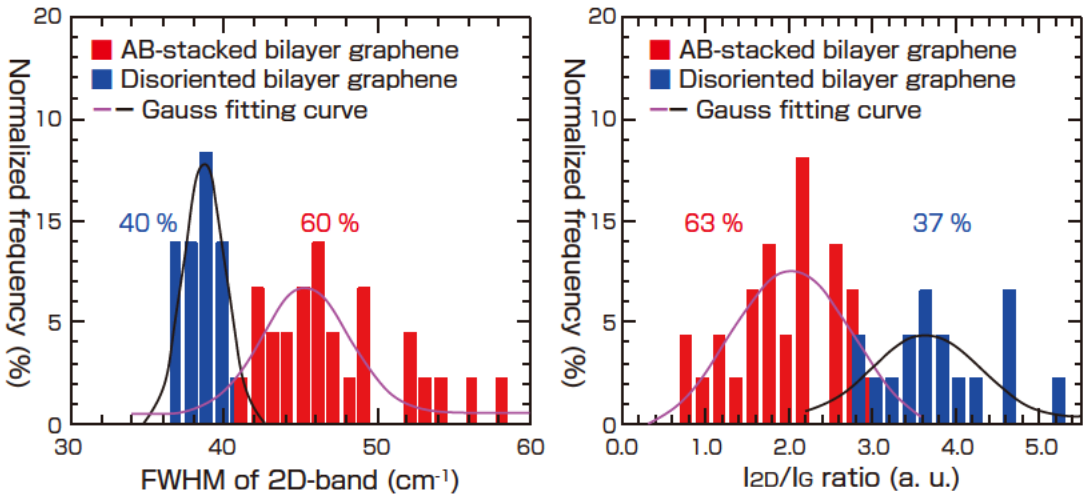

Fig. 11 The histograms of FWHM values of 2D-band and intensity ration of 2D-band/G-band[14]
Red bar is AB-stacked bilayer graphene and blue bar is disorder-stacked bilayer graphene.
Copyright (2014), with permission from Elsevier

Table 1. Mobility, FWHM of 2D-band, yield of AB-stacked bilayer graphene[14]
Copyright (2014), with permission from Elsevier

Growth process (Substrate & temperature)	Mobility (cm^2/Vs)	FWHM of 2D-band for AB-stacked (cm^{-1})	Yield of AB-stacked (%) [Yield of disoriented (%)]	Reference
Cu(25 μm), 1050 ℃	1500-4400	47.4-62.0	90[10]	L.Liu *et al.*,*ACS Nano*.6, 8241(2012)
Cu(25 μm), 1000 ℃	350-400	—	67*1	K. Yan *et al.*,*Nano Lett.*11,6(2011)
Cu(25 μm), 1000 ℃	580	45.0-53.0	99*2	S. Lee *et al.*,*Nano Lett.*10,4702(2010)
Cu(1.2 μm)-Ni(0.4 μm), 920 ℃	3485	38.0-50.0	98*3	W.Liu *et al.*,*Chem. Mater.*26,907(2014)
Cu(25 μm), 980 ℃	—	—	70[30]	L.Brown *et al.*,*Nano. Lett.*12,1609(2012)
Cu(6.3 μm), 850 ℃	1000	41-59.5	60[40]	This study

*1 Small amount of trilayer graphene was also observed.
*2 The rest of AB-stacked bilayer graphene was 32 % of single layer graphene.
*3 The amount of trilayer graphene was 1 %.

of a slightly-adhesive resin film (a), a graphene/slightly-adhesive resin film (b) and the ratio spectrum of only graphene (c) which is calculated by dividing (a) by (b). The optical transmittance of the slightly-adhesive resin film was 91.5 % and the graphene/slightly adhesive resin film was 86.4 % at wavelength of 550 nm. The only graphene film transmittance was 94.5 % at wavelength of 550 nm. It was found that the layer number corresponded to 2 layers estimated from 2.3 % transmittance loss of single layer graphene.[49]

The reported values of the mobility of bilayer graphene are listed together with the yield, synthesis temperature, and FWHM of AB-stacked bilayer graphene in Table 1.

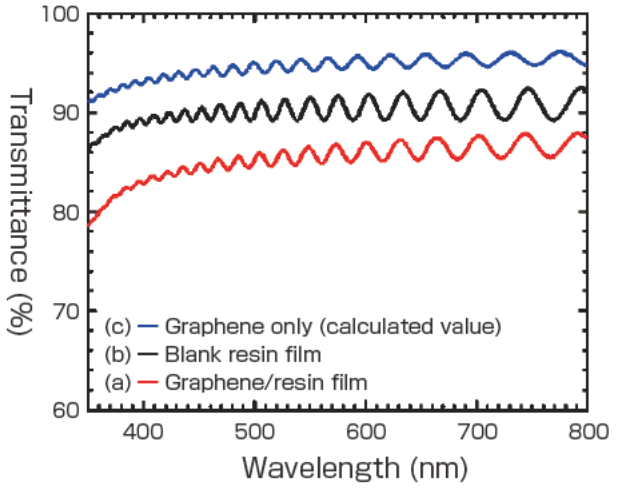

Fig. 12 Optical transmittance of base resin film and graphene/resin films[14]
Transmittance of graphene only (c) is calculated by dividing graphene/resin film (a) by blank resin film (b). Interference fringes of (a) and (b) are due to a very thin resin film.
Copyright (2014), with permission from Elsevier

In this study, the synthesis temperature is lower and the synthesis time is shorter compared to past reported values. However, the carrier mobility of 1000 cm^2/Vs obtained at room temperature showed significant improvement from the one around 100 cm^2/Vs[13] for previous plasma CVD. Higher mobility values than ours have been reported by Liu *et al.* of 1500–4400 cm^2/Vs[48] and Liu et al. of 3845 cm^2/Vs.[50] It is considered that the quality of bilayer graphene synthesized by plasma CVD can be improved further.

The sheet resistance of synthesized graphene was 951 Ω on average in this study. This sample was doped by gold chloride. Figure 13 shows the sheet resistance map after being doped by gold chloride. As shown in Fig. 13, the average sheet resistance of a 6 × 6 mm^2 sheet was 130 Ω and the lowest sheet resistance was less than 100 Ω.

By the development of plasma CVD using ultralow carbon

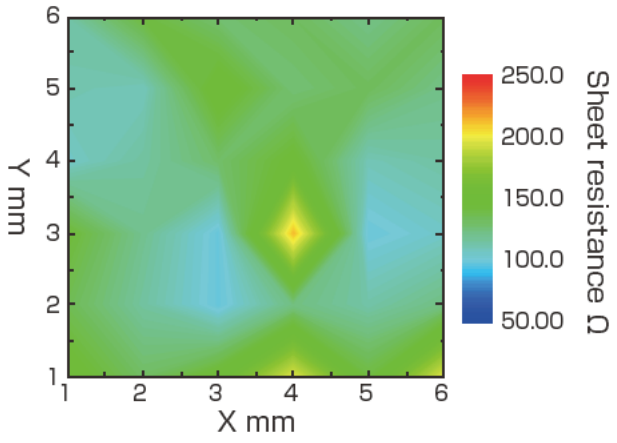

Fig. 13 The sheet resistance map of graphene after wet doping with gold chloride[14]
Copyright (2014), with permission from Elsevier

source, the crystalline quality of synthesized graphene was significantly improved, and the controllability of the number of layers was also improved. As carbon sources for graphene synthesis, we utilized trace amount of carbon contained in the copper foil and carbon supplied from the environment in the reaction chamber. Graphene of 60 % AB-stacked bilayer graphene and 40 % of disoriented bilayer graphene was synthesized. The sheet resistance of bilayer graphene was 951 Ω on average, and the carrier mobility was 1000 cm^2/Vs at room temperature. The sheet resistance of 130 Ω was attained after doping with a gold chloride solution.

4 The development of large area graphene synthesis technology

We attempted to synthesize A4 size large area graphene by combining plasma treatment and joule heating using ultralow carbon sources developed in this study. Figure 14 shows an A4 size large area graphene transparent conductive film which was synthesized on a copper foil substrate using the above method and then transferred onto a PET film. The optical transmittance of only graphene was 92 % (3.6 layers) and the sheet resistance was less than 500 Ω without doping. In this way, we succeeded in fabricating a A4 size large area graphene transparent conductive film using plasma treatment of ultralow carbon sources developed in this study.

5 The relationship between Hall mobility and crystalline quality

We examined the correspondence between Hall mobility and crystalline quality by Raman spectroscopy measurements of van der Pauw devices which measured the Hall mobility. Here, the Raman intensity ratio of the D-band and the G-band was an index for graphene crystalline quality. The relationship between the Hall mobility and the intensity ratio of the D-band/G-band is shown in Fig. 15. In this study, we prepared two graphene films. One was synthesized by plasma CVD using methane and hydrogen gas, the other was synthesized by combining plasma treatment and the joule heating method without using methane gas carried out in this study. In the case of plasma CVD of the previous method, the intensity ratio of the D-band/G-band was higher and mobility was 10–100 cm^2/Vs. On the other hand, in the case of the novel method, the intensity of the D-band/G-band was lower and mobility was 100–1000 cm^2/Vs, and we succeeded in achieving 10 times larger electric conductivity than the previous method. From the intensity ratio of Raman signals of the D-band and the G-band, it was possible to estimate the graphene domain size.[51] In the case of plasma CVD of the previous method, the estimated graphene domain size was 17 nm. On the other hand, in the case of the novel method which combined hydrogen plasma treatment and joule heating, it was 170 nm. Also from this result, we confirmed that the domain size had expanded to 10 times larger than the previous method.

6 Estimation of domain size by dark-field TEM

To directly estimate the domain size of the synthesized graphene film by plasma treatment of this study, we measured the graphene film by dark-field TEM. Graphene samples transferred to a TEM grid using polymethyl methacrylate (PMMA) were prepared. Figure 16(a) shows a bright-field TEM image, and Fig. 16(b) shows the selected area electron diffraction pattern (SAED). The graphene film seemed to be relatively uniform in the bright-field TEM image, but many family spots were observed in the SAED. The results suggest that several domains with different orientations exist. The

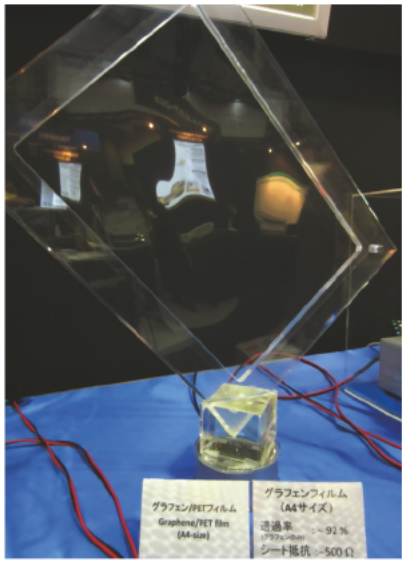

Fig. 14 A4 size large area graphene transparent conductive film
Transmittance : 92 % and sheet resistance : less than 500 Ω

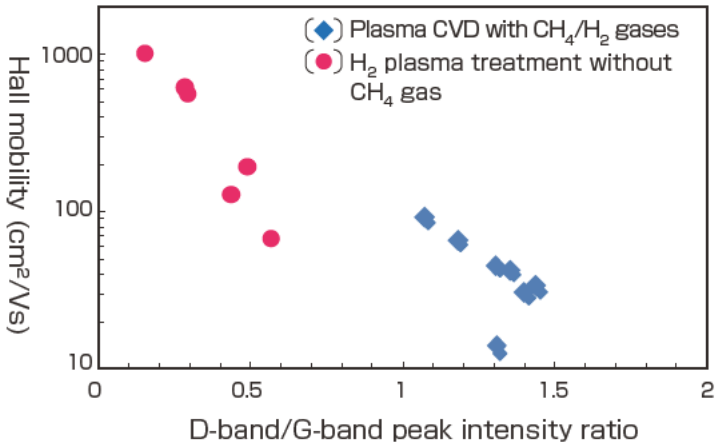

Fig. 15 The relationship between the Hall mobility and Raman intensity D-band/G-band ratio[15]
◆ Plasma CVD using CH_4/H_2 gas mixture, ● Hydrogen plasma treatment without CH_4 gas
Copyright (2015), with permission from Elsevier

Table 2. Comparison table of graphene synthesis by plasma CVD and thermal CVD

Plasma CVD	Thermal CVD
・Low temperature process ・Large area deposition (Deposition area increases by antenna) ・Wide layer control range ・High growth rate and continuous deposition ・High throughput (Integration of pretreatment and synthesis process) ・Low cost	・High temperature process ・Deposition area is limited by CVD furnace size ・Narrow layer control range ・Low growth rate ・Low throughput (Pretreatment and synthesis process are not integrated) ・High cost

dark-field TEM images of each spot are shown in Fig. 16(c) and (d). Both figures suggest that the domain size is about 100 nm, which is consistent with the domain size estimated from the Raman measurement.

7 Comparison of graphene synthesis by plasma CVD and thermal CVD

Finally, based on results obtained in this study, comparison of graphene synthesis by plasma CVD and thermal CVD methods is shown in Table 2.

8 Summary and Future Perspectives

In this paper, we reported the attempt of the establishment of high-throughput plasma-enhanced CVD for high-quality graphene. By using plasma CVD methods, we elucidated the mechanism of attaining high purity of the copper foil surface by He/H_2 plasma pretreatment and the suppression of silicon impurities from the quartz window. Furthermore, we developed a plasma CVD method using ultralow carbon sources for reduction of nucleation density, and the selective bilayer graphene synthesis was attained combining plasma CVD and joule heating. The grain size of graphene was expanded to 10 times and the Hall mobility was improved to 1000 cm^2/Vs.

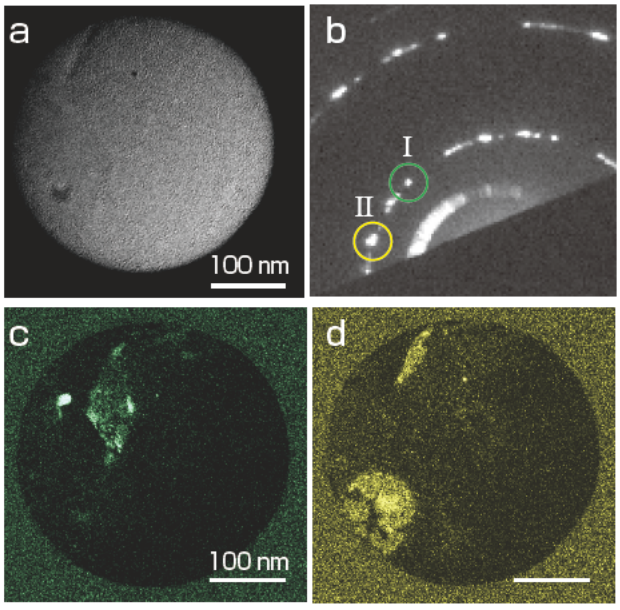

Fig. 16 (a) TEM image, (b) the selected area electron diffraction pattern, and (c) (d) The dark-field TEM images[15]
Copyright (2015), with permission from Elsevier

Though we did not mention in detail the difference between plasma CVD and thermal CVD in this paper, we have recently clarified the advantages of plasma CVD from the view point of reduction of process time and process temperature.[16]

In the near future, we want to push forward the establishment of a high-throughput plasma CVD method for high-quality and large-area graphene which exceeds the graphene quality synthesized by the main current high-temperature thermal CVD methods.

Acknowledgements

Part of the results was attained through the NEDO Project for "Basic Research and Development of Graphene."

References

[1] K. S. Novoselov, A. K. Geim, S. V. Morozov, D. Jiang, Y. Zhang, S. V. Dubonos, I. V. Grigorieva and A. A. Firsov: Electric field effect in atomically thin carbon films, *Science*, 306, 666–669 (2004).
[2] A. Kumar and C. Zhou: The race to replace tin-doped indium oxide: Which material will win?, *ACS Nano*, 4 (1), 11–14 (2010).
[3] A. K. Geim: Graphene: Status and prospects, *Science*, 324, 1530–1534 (2009).
[4] K.H. Liao, A. Mittal, S. Bose, C. Leighton, K. A. Mkhoyan and C. W. Macosko: Aqueous only route toward graphene from graphite oxide, *ACS Nano*, 5 (2), 1253–1258 (2011).
[5] C. Virojanadara, M. Syväjarvi, R. Yakimova, L. I. Johansson, A. A. Zakharov and T. Balasubramanian: Homogeneous large-area graphene layer growth on 6H-SiC(0001), *Phys. Rev.*, B 78, 245403-1–245403-6 (2008).
[6] X. Li, W. Cai, J. An, S. Kim, J. Nah, D. Yang, R. Piner, A. Velamakanni, I. Jung, E. Tutuc, S. K. Banerjee, L. Colombo and R. S. Ruoff: Large-area synthesis of high-quality and uniform graphene films on copper foils, *Science*, 324, 1312–1314 (2009).

[7] S. Bae, H. Kim, Y. Lee, X. Xu, J. S. Park, Y. Zheng, J. Balakrishnan, T. Lei, H. R. Kim, Y. I. Song, Y.J. Kim, K. S. Kim, B. Özyilmaz, J.H. Ahn, B. H. Hong and S. Iijima: Roll-to-roll production of 30-inch graphene films for transparent electrodes, *Nature Nanotechnology*, 5, 574–578 (2010).

[8] J. Kim, M. Ishihara, Y. Koga, K. Tsugawa, M. Hasegawa and S. Iijima: Low-temperature synthesis of large-area graphene-based transparent conductive films using surface wave plasma chemical vapor deposition, *Appl. Phys. Lett*., 98, 091502-1–091502-3 (2011).

[9] T. Yamada, M. Ishihara, J. Kim, M. Hasegawa and S. Iijima: A roll-to-roll microwave plasma chemical vapor deposition process for the production of 294 mm width graphene films at low temperature, *Carbon*, 50, 2615–2619 (2012).

[10] T. Yamada, J. Kim, M. Ishihara and M. Hasegawa: Low-temperature graphene synthesis using microwave plasma CVD, *J. Phys. D: Appl. Phys*., 46, 063001–063008 (2013).

[11] T. Yamada, M. Ishihara and M. Hasegawa: Low temperature graphene synthesis from poly(methyl methacrylate) using microwave plasma treatment, *Appl. Phys. Express*, 6, 115102-1–115102-3 (2013).

[12] Y. Okigawa, K. Tsugawa, T. Yamada, M. Ishihara and M. Hasegawa: Electrical characterization of graphene films synthesized by low-temperature microwave plasma chemical vapor deposition, *Appl. Phys. Lett*., 103, 153106-1–153106-4 (2013).

[13] R. Kato, K. Tsugawa, T. Yamada, M. Ishihara and M. Hasegawa: Improvement of multilayer graphene synthesis on copper substrate by microwave plasma process using helium at low temperatures, *Jpn. J. Appl. Phys*., 53, 015505-1–015505-6 (2014).

[14] R. Kato, K. Tsugawa, Y. Okigawa, M. Ishihara, T. Yamada and M. Hasegawa: Bilayer graphene synthesis by plasma treatment of copper foils without using a carbon-containing gas, *Carbon*, 77, 823–828 (2014).

[15] Y. Okigawa, R. Kato, T. Yamada, M. Ishihara and M. Hasegawa: Electrical properties and domain sizes of graphene films synhesized by microwave plasma treatment under a low carbon concentration, *Carbon*, 82, 60–66 (2015).

[16] R. Kato, S. Minami, Y. Koga and M. Hasegawa: High growth rate chemical vapor deposition of graphene under low pressure by RF plasma assistance, *Carbon*, 96, 1008–1013 (2016).

[17] Z. Luo, Y. Lu, D. W. Singer, M. E. Berck, L. A. Somers, B. R. Goldsmith and A. T. C. Johnson: Effect of substrate roughness and feedstock concentration on growth of wafer-scale graphene at atmospheric pressure, *Chem. Mater.*, 23, 1441–1447 (2011).

[18] G. H. Han, F. Günes, J. J. Bae, E. S. Kim, S. J. Chae, H. -J. Shin, J. Y. Choi, D. Pribat and Y. H. Lee: Influence of copper morphology in forming nucleation seeds for graphene growth, *Nano Lett*., 11, 4144–4148 (2011).

[19] M. L. Hartenstein, S. J. Christopher and R. K. Marcus: Evaluation of helium-argon mixed gas plasmas for bulk and depth-resolved analyses by radiofrequency glow discharge atomic emission spectroscopy, *J. Anal. At. Spectrom*., 14, 1039–1048 (1999).

[20] P. Sigmund: Theory of sputtering. I. Sputtering yield of amorphous and polycrystalline targets, *Phys. Rev.*, 184, 383–416 (1969).

[21] D-H. Kim, G-H. Lee, S. Y. Lee and D. H. Kim: Atomic scale simulation of physical sputtering of silicon oxide and silicon nitride thin films, *J. Cryst. Growth*, 286, 71–77 (2006).

[22] H. Sugai, I Ghanashev and M. Nagatsu: High-density flat plasma production based on surface waves, *Plasma Sources Sci. Technol*., 7, 192–205 (1998).

[23] H. Sugai, I. Ghanashev and K. Mizuno: Transition of electron heating mode in a planar microwave discharge at low pressures, *Appl. Phys. Lett*., 77 (22), 3523–3525 (2000).

[24] K. Tsugawa, M. Ishihara, J. Kim, M. Hasegawa and Y. Koga: Large-area and low-temperature nanodiamond coating by microwave plasma chemical vapor deposition, *New Diamond Front. Carbon Technol*., 16 (6), 337–346 (2006).

[25] K. Tsugawa, M. Ishihara, J. Kim, Y. Koga and M. Hasegawa: Nanocrystalline diamond film growth on plastic substrates at temperatures below 100 °C from low-temperature plasma, *Phys. Rev*., B82, 125460-1–125460-8 (2010).

[26] J. Kim, K. Tsugawa, M. Ishihara, Y. Koga and M. Hasegawa: Large-area surface wave plasmas using microwave multi-slot antennas for nanocrystalline diamond film deposition, *Plasma Sources Sci. Technol*., 19, 015003-1–015003-5 (2010).

[27] K. Tsugawa, S. Kawaki, M. Ishihara, J. Kim, Y. Koga, H. Sakakita, H. Koguchi and M. Hasegawa: Nanocrystalline diamond growth in surface-wave plasma, *Diamond & Related Materials*, 20, 833–838 (2011).

[28] Z. H. Gan, G. Q. Yu, B. K. Tay, C. M. Tan, Z. W. Zhao and Y. Q. Fu: Preparation and characterization of copper oxide thin films deposited by filtered cathodic vacuum arc, *J. Phys. D: Appl. Phys*., 37 (1), 81–85, (2004).

[29] J. Ghijsen, L. H. Tjeng, J. van Elp, H. Eskes, J. Westerink, G. A. Sawatzky and M. T. Czyzyk: Electronic structure of Cu_2O and CuO, *Phys. Rev*., B 38, 11322–11330 (1988).

[30] C. C. Chusuei, M. A. Brookshier and D. W. Goodman: Correlation of relative X-ray photoelectron spectrscopy shake-up intensity with CuO particle size, *Langmuir*, 15, 2806–2808 (1999).

[31] B. Balamurugan, B. R. Mehta and S. M. Shivaprasad: Surface-modified CuO layer in size-stabilized single-phase Cu_2O nanoparticles, *Appl. Phys. Lett*., 79 (19), 3176–3178 (2001).

[32] M. Yin, C-K. Wu, Y. Lou, C. Burda, J. T. Koberstein, Y. Zhu and S. O'Brien: Copper oxide nanocrystals, *J. Am. Chem. Soc*., 127, 9506–9511 (2005).

[33] S. K. Chawla, N. Sankarraman and J. H. Payer: Diagnostic spectra for XPS analysis of Cu-O-S-H compounds, *J. Electr. Spectrosc. Relat. Phenom*., 61, 1–18 (1992).

[34] B. Schnyder, T. Lippert, R. Kötz, A. Wokaun, V-M. Graubner and O. Nuyken: UV-irradiation induced modification of PDMS films investigated by XPS and spectroscopic ellipsometry, *Surf. Sci*., 532–535, 1067–1071 (2003).

[35] L-A. O'Hare, A. Hynes and M. R. Alexander: A methodology for curve-fitting of the XPS Si 2*p* core level from thin siloxane coatings, *Surf. Inter. Analy*., 39, 926–936 (2007).

[36] J-H. Lin, H-C. Chiu, Y-R. Lin, T-K. Wen, R. A. Patil, R. S. Devan, C-H. Chen, H-W. Shiu, Y. Liou and Y-R. Ma: Electrical and chemical chracteristics of probe-induced two-dimensional SiO_X protrusion layers, *Appl. Phys. Lett*., 102, 031603-1–031603-5 (2013).

[37] M. J. Webb, P. Palmgren, P. Pal, O. Karis and H. Grennberg: A simple method to produce almost perfect graphene on highly oriented pyrolytic graphite, *Carbon*, 49, 3242–3249 (2011).

[38] M. Finšgar, J. Kovač and I. Milošev: Surface analysis of 1-hydroxybenzotriazole and benzotriazole adsorbed on Cu by X-ray photoelectron spectroscopy, *J. Electrochem. Soc*.,

157, C52–C60 (2010).
[39] R. M. Souto, V. Fox, M. M. Laz, M. Pérez and S. González: Some experiments regarding the corrosion inhibition of copper by benzotriazole and potassium ethyl xanthate, *J. Electroanaly. Chem*., 411, 161–165 (1996).
[40] H. Kinoshita, M. Umeno, M. Tagawa and N. Ohmae: Hyperthermal atomic oxygen beam-induced etching of HOPG (0001) studied by X-ray photoelectron spectroscopy and scanning tunneling microscopy, *Surf. Sci*., 440, 49–59 (1999).
[41] T. Terasawa and K. Saiki: Growth of graphene on Cu by plasma enhanced chemical vapor deposition, *Carbon*, 50, 869–874 (2012).
[42] T-H. Han, Y. Lee, M-R. Choi, S-H. Woo, S-H. Bae, B. H. Hong, J-H. Ahn and T-W. Lee: Extremely efficient flexible organic light-emitting diodes with modified graphene anode, *Nat. Photon*., 6, 105–110 (2012).
[43] T. Kobayashi, M. Bando, N, Kimura, K. Shimizu, K. Kadono, N. Umezu, K. Miyahara, S. Hayazaki, S. Nagai, Y. Mizuguchi, Y. Murakami and D. Hobara: Production of a 100-m-long high-quality graphene transparent conductive film by roll-to-roll chemical vapor deposition and transfer process, *Appl. Phys. Lett*., 102, 023112-1–023112-4 (2013).
[44] L. J. van der Pauw: A method of measuring specific resistivity and Hall effect of discs of arbitrary shape, *Philips Res. Repts*., 13, 1–9 (1958).
[45] J. Robertson: Diamond-like amorphous carbon, *Mater. Sci. Eng*., R37, 129–281 (2002).
[46] L. G. Cançado, A. Reina, J. Kong and M. S. Dresselhaus: Geometrical approach for the study of *G'* band in the Raman spectrum of monolayer graphene, bilayer graphene, and bulk graphite, *Physical Review*, B77, 245408-1–245408-9 (2008).
[47] A. C. Ferrari, J. C. Meyer, V. Scardaci, C. Casiraghi, M. Lazzeri, F. Mauri, S. Piscanec, D. Jiang, K. S. Novoselov, S. Roth and A. K. Geim: Raman spectrum of graphene and graphene layers, *Phys Rev Lett*., 97, 187401-1–187401-4 (2006).
[48] L. Liu, H. Zhou, R. Cheng, W. J. Yu, Y. Liu, Y. Chen, J. Shaw, X. Zhong, Y. Huang and X. Duan: High-yield chemical vapor deposition growth of high-quality large-area AB-stacked bilayer graphene, *ACS Nano*., 6, 8241–8249 (2012).
[49] R. R. Nair, P. Blake, A. N. Grigorenko, K. S. Novoselov, T. J. Booth, T. Stauber, N. M. R. Peres and A. K. Geim: Fine structure constant defines visual transparency of graphene, *Science*, 320, 1308 (2008).
[50] W. Liu, S. Kraemer, D. Sarker, H. Li, P. M. Ajayan and K. Banerjee: Controllable and rapid synthesis of high-quality and large-area Bernal stacked bilayer graphene using chemical vapor deposition, *Chem. Mater.*, 26, 907–915 (2014).
[51] L. G. Cançado, K. Takai, T. Enoki, M. Endo, Y. A. Kim, H. Mizusaki, A. Jorio, L. N. Coelho, R. M.-Paniago and M. A. Pimenta: General equation for the determination of the crystallite size L_a of nanographite by Raman spectroscopy, *Appl. Phys. Lett*., 88, 163106-1–163106-3 (2006).

Authors

Masataka HASEGAWA
Completed the doctor's program at the Graduate School of Engineering, Kyoto University in 1990. Joined the Electrotechnical Laboratory, Agency of Industrial Science and Technology in 1990. Currently, Group Leader, Carbon-Based Thin Film Materials Group, Nanomaterials Research Institute, AIST. General Manager, Graphene Division Project Headquarters, Technology Research Association for Single Wall Carbon Nanotubes (TASC) from 2011 to present. Engages in the R&D for electroconductivity control of diamond semiconductor, CVD growth on monocrystal diamond, CVD synthesis of nanocrystal diamond thin film, and CVD synthesis for graphene. In this paper, was in charge of overseeing the overall research topics and the development of plasma CVD device for graphene and its synthesis method.

Kazuo TSUGAWA
Graduated from the Department of Electronics and Communication Engineering, School of Science and Engineering, Waseda University in 1992. Withdrew from the doctor's program at the Department of Electronics, Information and Communication Engineering, Graduate School of Science and Engineering, Waseda University in 1998. Assistant, School of Science and Engineering, Waseda University from 1998 to 2000. Researcher, Japan Fine Ceramics Center from 2000 to 2003; Postdoctoral Fellow and Technical Staff at the Research Center for Advanced Carbon Materials, Nanocarbon Research Center, and CNT Application Research Center, AIST from 2003 to 2011; and Researcher, Graphene Division, Technology Research Association for Single Wall Carbon Nanotubes from 2010 to 2013. Part-time Lecturer, Faculty of Science and Engineering, Waseda University from 2010 to 2013. Application Manager, Seki Diamond Systems, Cornes Technologies Ltd. from 2013 to present. Doctor (Engineering). In this paper, was in charge of the CVD synthesis of graphene and its evaluation.

Ryuichi KATO
Graduated from the College of Engineering Sciences, University of Tsukuba in 2008. Withdrew from the master's course at the Department of Materials Science, Graduate School of Pure and Applied Sciences, University of Tsukuba in 2011. Currently enrolled in the doctor's program at the Department of Materials Science, Graduate School of Pure and Applied Sciences, University of Tsukuba. Researcher, Graphene Division, Technology Research Association for Single Wall Carbon Nanotubes (TASC) from 2011 to present. In this paper, was in charge of the development of plasma pretreatment technology for graphene copper substrate using helium, and the synthesis and analysis of double-layered graphene using low-concentration carbon source.

Yoshinori KOGA
Graduated from the Department of Applied Chemistry, Faculty of Science and Engineering, Waseda University in 1969. Withdrew from the doctor's program at the Department of Applied Chemistry, Graduate School of Science and Engineering, Waseda University in 1974. Joined the Government Chemical Industrial Research Institute, Tokyo, Agency of Industrial Science and Technology in 1974. Doctor (Science) in 1974. Deputy Manager, Planning Office and Section Chief, Polymer Analysis Section, National Chemical Laboratory for Industry. Manager of Molecular Measurement Laboratory and Manager of Laser Reaction Lab, National Institute of Materials and Chemical Research in 1993. Deputy Director, Research Center for Advanced Carbon Materials, AIST from 2001 to 2008. Part-time Lecturer, Graduate School of Science and Technology, Nihon University from 2010 to 2014; and Part-time Lecturer, Graduate School of Engineering, Mie University from 2015 to present. Researcher, Graphene Division, Technology Research Association for Single Wall

Carbon Nanotubes (TASC) from 2011 to present. In this paper, was in charge of the plasma analysis and double-layered graphene analysis.

Masatou ISHIHARA
Graduated from the Department of Industrial Chemistry (currently Pure and Applied Chemistry), Faculty of Science and Technology, Tokyo University of Science in 1991. Researcher, Research Department, Kurami Works, Nippon Mining and Metals Co., Ltd. (currently JX Nippon Mining and Metals Corporation). Completed the doctor's program at the Department of Materials Science and Technology, Graduate School of Industrial Science and Technology, Tokyo University of Science in 1997. Doctor (Engineering). Postdoctoral Fellow, Japan Science and Technology Agency in 1997. Joined the National Institute of Materials and Chemical Research, Agency of Industrial Science and Technology in 2000. Researcher, Research Center for Advanced Carbon Materials, AIST in 2001. Senior Researcher, Carbon-Based Thin Film Materials Group, Nanomaterials Research Institute, AIST from 2015 to present. In this paper, was in charge of the substrate pretreatment by wet method, the transfer of graphene to transparent substrate, the development of use of transparent conductive films, and others.

Takatoshi YAMATAKA
Graduated from the Department of Electronics, School of Engineering, Tokai University in 1996. Completed the master's program at the Department of Electronics, Graduate School of Engineering, Tokai University in 1998. Assistant, College of Science and Engineering, Aoyama Gakuin University in 1998. Assistant, Institute of Multidisciplinary Research for Advanced Materials, Tohoku University in 2003. Joined AIST in 2004. Currently, Senior Researcher, Carbon-Based Thin Film Materials Group, Nanomaterials Research Institute. In this paper, was in charge of the impurity analysis for plasma CVD graphene and the evaluation of electrical characteristics.

Yuki OKIGAWA
Graduated from the Department of Electrical Electronic Engineering and Information Engineering, School of Engineering, Nagoya University in 2007. Completed the doctor's program at the Department of Quantum Science and Energy Engineering, Graduate School of Engineering, Nagoya University in 2012. Doctor (Engineering). Joined the CNT Application Research Center, AIST in 2012. Currently, Researcher, Carbon-Based Thin Film Materials Group, Nanomaterials Research Institute. In this paper, was in charge of the fabrication of device using graphene and the evaluations of electroconductivity characteristic and crystallization property of the device.

Discussions with Reviewers

1 Overall

Comment (Shuji Abe, Musashino University)

This paper is very convincing as it experimentally investigates details of plasma CVD synthesis technology for graphene developed by the authors employing various original ideas, and then it empirically describes high quality graphene synthesis that has become possible through such efforts.

Comment (Hiroaki Hatori, AIST)

The technology that enables high-quality, high-speed, and large-area synthesis of graphene is the key in the realization of long-awaited transparent electrodes, and I think it is very interesting to see a discussion of such a technological development process in a synthesiological light. This paper is significant in that it shows the course of R&D for the establishment of high-quality high-throughput synthesis technology for graphene transparent conductive films using plasma CVD.

2 Prospects for industrial production

Question and Comment (Shuji Abe)

The "ultralow carbon concentration plasma CVD" does not use carbon-containing gas at all, and the materials for graphene are the carbon supplied from the impurities in copper foil and environment inside the reaction chamber, but these are factors that cannot be controlled by engineering. Certainly, we see that the crystal size is improved and the plasma treatment time is shortened in the laboratory, but do you have prospect toward industrial production?

Answer (Masataka Hasegawa)

Since it has become clear that the improvement of crystal size is due to the reduction of nucleus formation site in ultralow carbon concentration, monitoring the impurities in the production process is important, and forming good quality graphene films by reducing the number of nucleus formation sites is extremely important in future industrial processes. Therefore, the supply of excessive carbon reduces the quality of graphene, and impurity monitoring from the reaction chambers and others will be necessary in the industrial production. Currently, we are conducting an A4-size bench scale experiment, and continuous supply of carbon sources at optimal concentration will become necessary for large-scale continuous film forming.

3 Technological selection for achieving the goal

Question and Comment (Hiroaki Hatori)

In this paper, the background of development, the scenario, and the results based on this scenario are summarized for each elemental technology including the solution for impurity incorporation, the improvement of quality by reduction of graphene nucleus formation density, and the development of selective synthesis of double-layered graphene. Ultimately, you succeeded in the synthesis of a large-area transparent graphene conductive film. On the other hand, from the perspective of technological selection toward the final goal of realizing the transparent graphene electrode, I think the readers will better understand the overall scenario by which the authors achieved success in developing the large-area transparent graphene conductive film if you discuss the differences of your technology against the thermal CVD method that you mention partially in this paper, and make contrasts with other competing technologies.

Answer (Masataka Hasegawa)

We created and inserted a table comparing the plasma CVD and the conventional thermal CVD in Chapter 7, to allow easy understanding of the superiority of the high-throughput plasma CVD method.